

Analysis of the $^{168}\text{Er}(d, t)^{167}\text{Er}$ reaction at 17 MeV†

H. S. Song,* J. J. Kolata,‡ and J. V. Maher

University of Pittsburgh, Pittsburgh, Pennsylvania 15260

(Received 9 May 1977)

Angular distributions have been measured for transitions populating residual states of ^{167}Er through the $^{168}\text{Er}(d, t)$ reaction at $E_d = 17$ MeV. Many of these angular distributions have shapes which are well reproduced by distorted-wave Born-approximation calculations. A small but significant number of angular distributions are anomalous; i.e., either they do not resemble any reasonable distorted-wave Born-approximation calculation or they can only be fitted with a calculation which assumes an l value incompatible with the previous Nilsson model assignment for the residual state. While the summed spectroscopic factors are in good agreement with Nilsson model expectations, there is considerable evidence of fragmentation of the single-quasihole strength and the spectroscopic factors for several levels deviate significantly from Nilsson model predictions, even though Coriolis coupling has been included in the model calculation. The observation of several strongly anomalous angular distributions almost certainly indicates that the assumption of a simple one-step direct reaction mechanism breaks down for some of these transitions. The discrepancies between the model prediction and the experimental spectroscopic factors could arise either from a multistep mechanism or from mixing of the simple quasihole states with more complicated states of the same spin-parity. The observed fragmentation of strength is strong evidence for such mixing.

[NUCLEAR REACTIONS $^{168}\text{Er}(d, t)$, $E_d = 17$ MeV measured $\sigma(\theta)$; DWBA analysis; deduced levels, l values, spectroscopic factors. Enriched targets.]

I. INTRODUCTION

The limits of applicability of the direct single-step reaction assumption are not well established and the investigation of these limits has motivated many recent investigations.¹⁻³ Unfortunately, since distorted-wave Born-approximation (DWBA) calculations are easily performed and the next most reasonable improvement—the coupled-channels Born approximation (CCBA) calculation—is much more difficult to perform, there has been a tendency to vary parameters to fit as much data as possible with DWBA and to apply CCBA only in an *ad hoc* fashion to troublesome cases of experimental data. This difficulty in defining the limits of applicability of the DWBA is exacerbated by problems of acquiring a data base. Multinucleon transfer reactions frequently stretch the DWBA assumptions, but for such reactions it is not possible to separate structure from kinematic factors in the DWBA calculations so the analysis procedure is less reliable than for single-nucleon transfer reactions where structure and kinematic factors are algebraically separable. On the other hand, multistep effects in single-nucleon transfer reactions appear to be small for most cases of spherical nuclides. The study of (d, t) reactions on deformed rare-earth targets provides an excellent opportunity to acquire an extensive set of data for which the DWBA assumption should be marginal and for which the DWBA analysis should be reasonably straightforward. Both the deuteron and

the triton are strongly absorbed and, at least for most transitions in spherical nuclides, (d, t) angular distributions have smooth diffraction patterns which are easily fitted with DWBA calculations that use reasonable optical model parameter sets. The splitting of single-particle states in deformed nuclei provides, in any one deformed residual nucleus, a multiplicity of states of each spin. For most of these states direct single-particle transfer amplitudes are sufficiently small that multistep effects might be detectable.^{5,6}

This work is part of a larger investigation into the spectroscopy of the deformed rare-earth region and the mechanism of the (d, t) reaction in this mass region. In one previous paper⁷ it was shown that, when the (d, t) reaction is initiated by 17 MeV deuterons, the angular distribution shapes are unambiguously characteristic of orbital angular momentum transfer (l) over the entire range $0 \leq l \leq 6$. Another report⁸ presented evidence for systematic violations of one-step direct reaction assumptions in transitions populating certain single-particle states in the even-even targets ^{160}Gd , $^{162,164}\text{Dy}$, and $^{166,168}\text{Er}$. DWBA analysis of the observable transitions to members of the $\frac{1}{2}^-$ [505], $\frac{3}{2}^-$ [521], $\frac{1}{2}^-$ [521], and $\frac{5}{2}^+$ [642] Nilsson bands shows anomalous spectroscopic factors and/or anomalous angular distribution shapes for transitions to some members of each of these bands in nearly all residual nuclides which were studied. The transitions discussed in Ref. 8 were restricted to low-lying states of reasonably well established spin-parity

where there is no doubt of expected orbital angular momentum transfer (l) and where unaccounted vibrational couplings should have minimum effects on Nilsson model predictions of single-particle strengths. Recent papers^{9,10} in this series presented both reaction mechanism and spectroscopic results for all the observed transitions in the study of the (d, t) reaction on the $N=96$ isotones, ^{160}Gd , and ^{162}Dy , and the $N=98$ isotones, ^{164}Dy and ^{166}Er .

This paper presents the detailed results of an investigation of the (d, t) reaction at 17 MeV on the $N=100$ nucleus ^{168}Er . (d, p) and (d, t) spectra for this nucleus^{11,12} have been measured at lower beam energy (12 MeV), but no angular distributions have been reported previously. ^{167}Er has also been studied by Coulomb excitation,¹² neutron capture,¹⁴ and through its population in the $^{168}\text{Er}(^3\text{He}, \alpha)$ reaction¹⁵ (again without angular distributions).

The data of the present investigation have been analyzed with finite range nonlocal DWBA calculations. The intent of this analysis is to organize the data for comparison with Nilsson model expectations as to orbital angular momentum transfer (l) and spectroscopic strength. Since, between the Nilsson model and the DWBA calculations there are many possible parameters which could be varied, an attempt has been made to standardize the analysis parameters with the best available infor-

mation rather than make *ad hoc* parameter variations to fit data for individual transitions.

II. DATA ACQUISITION AND REDUCTION

The experiment was performed with 17 MeV deuterons from the Pittsburgh three stage Van de Graaff accelerator. The targets were $\sim 75 \mu\text{g}/\text{cm}^2$ foils of erbium oxide (Er_2O_3 , enriched to 97.7% in ^{168}Er) evaporated on carbon backings. Tritons from the (d, t) reaction were detected in photographic emulsions placed in the focal plane of a split-pole spectrograph. The spectrograph entrance aperture subtended a solid angle of 1.4 msr. The developed photographic plates were scanned by the Argonne automatic plate scanner¹⁶; some were checked by human scanners. A typical spectrum is shown in Fig. 1. The overall energy resolution is approximately 11 keV. Measurements were made for this reaction at 18 angles over the range $8^\circ \leq \theta_{\text{lab}} \leq 60^\circ$. Two NaI detectors were set at $\theta_{\text{lab}} = \pm 38^\circ$ to monitor possible target deterioration. Peak areas were extracted from the spectra with the peak-fitting code AUTOFIT.¹⁷ The reliability of the fitting procedure was monitored with numerous hand checks.

Angular distributions have been measured for the elastic scattering of 17 MeV deuterons from ^{168}Er , and other rare-earth targets [this and the

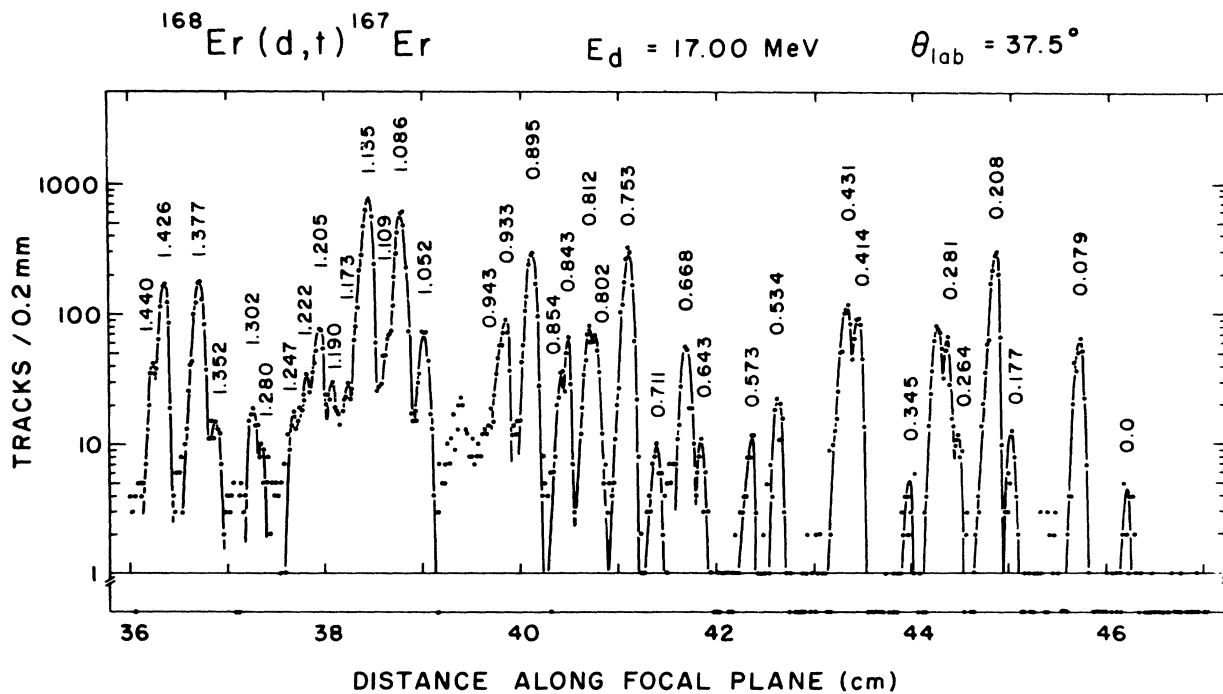


FIG. 1. Spectrum of tritons from the $^{168}\text{Er}(d, t)^{167}\text{Er}$ reaction measured at $\theta_{\text{lab}} = 37.5^\circ$. Excitation energies of residual ^{167}Er state are listed in MeV.

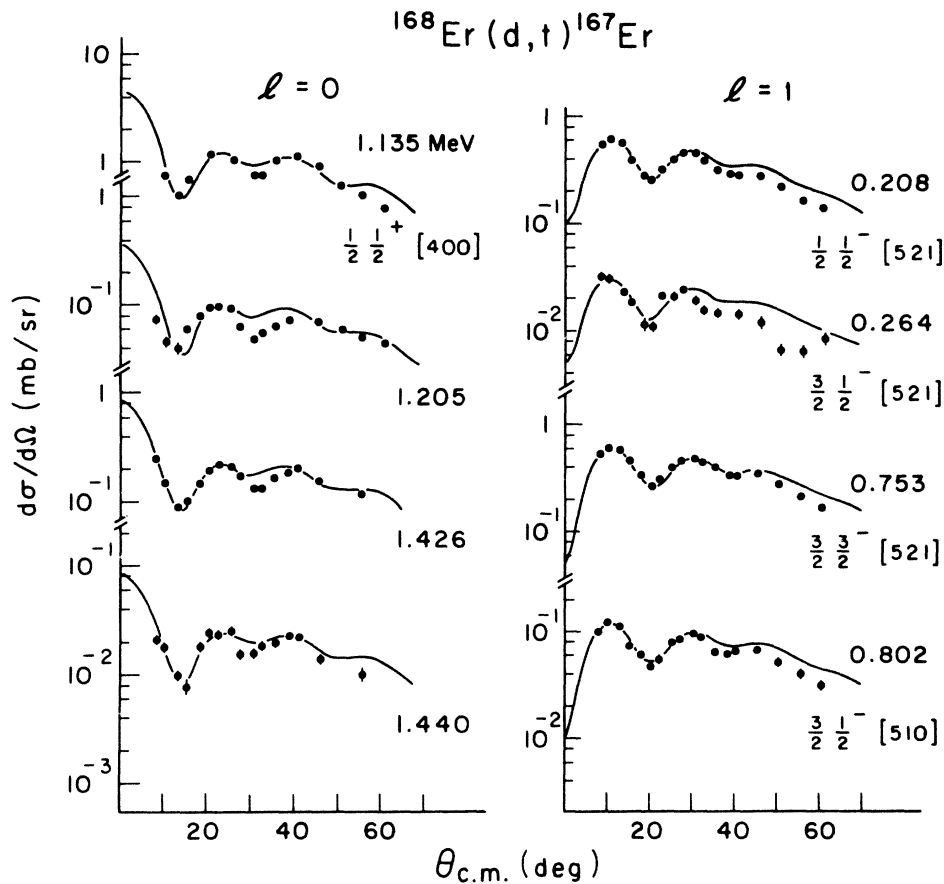


FIG. 2. $l=0$ and 1 angular distributions from the $^{168}\text{Er}(d,t)^{167}\text{Er}$ reaction at $E_d=17$ MeV. The solid curves are DWBA calculations.

results of an optical model analysis have been reported previously along with the results of the ^{160}Gd and $^{162}\text{Dy}(d,t)$ reactions⁹. Since the elastic scattering cross sections were thus established, it was possible to use the yields from the NaI monitor detectors to extract absolute cross sections (which should be accurate to $\pm 15\%$). The measured angular distributions of $^{168}\text{Er}(d,t)^{167}\text{Er}$ reactions are shown in Figs. 2-5.

III. DWBA CALCULATIONS AND ANGULAR DISTRIBUTION SHAPES

The code DWUCK¹⁸ was used to perform the finite range nonlocal DWBA calculations described in this section. Table I lists the optical potential parameters and bound state potential parameters used in these calculations. The finite range parameter was set at 0.845 and the nonlocality parameters at 0.54 (for the deuteron) and 0.25 (for the triton). The triton optical potential are those of Flynn *et al.*¹⁹ while the deuteron optical poten-

tial comes from the global search of Perey and Perey.²⁰ For a complete description of these DWBA calculations, including discussions of choice of optical potential^{21,22} and selection of quantum numbers for the bound state form factor,²³ see Ref. 9.

Angular distributions for most of the strong transitions observed in this experiment are well fitted by the DWBA predictions—as can be seen from Figs. 2-5. The strong $l=0$ angular distributions are extremely well fitted (Fig. 2). $l=2$ and $l=3$ angular distributions are also well fitted but, for weakly populated states, the angular distributions have a tendency to deviate from the predicted shapes; the experimental data show larger small-angle cross sections and minor oscillations of measured cross sections around the gross DWBA distribution shapes (Fig. 3). The $l \geq 4$ angular distributions are reasonably well fitted, but in addition to a tendency toward small-angle deviations like those of the $l=2,3$ distributions, some of them exhibit a small angular shift between measured and predicted angular distribution maxima (Fig. 4).

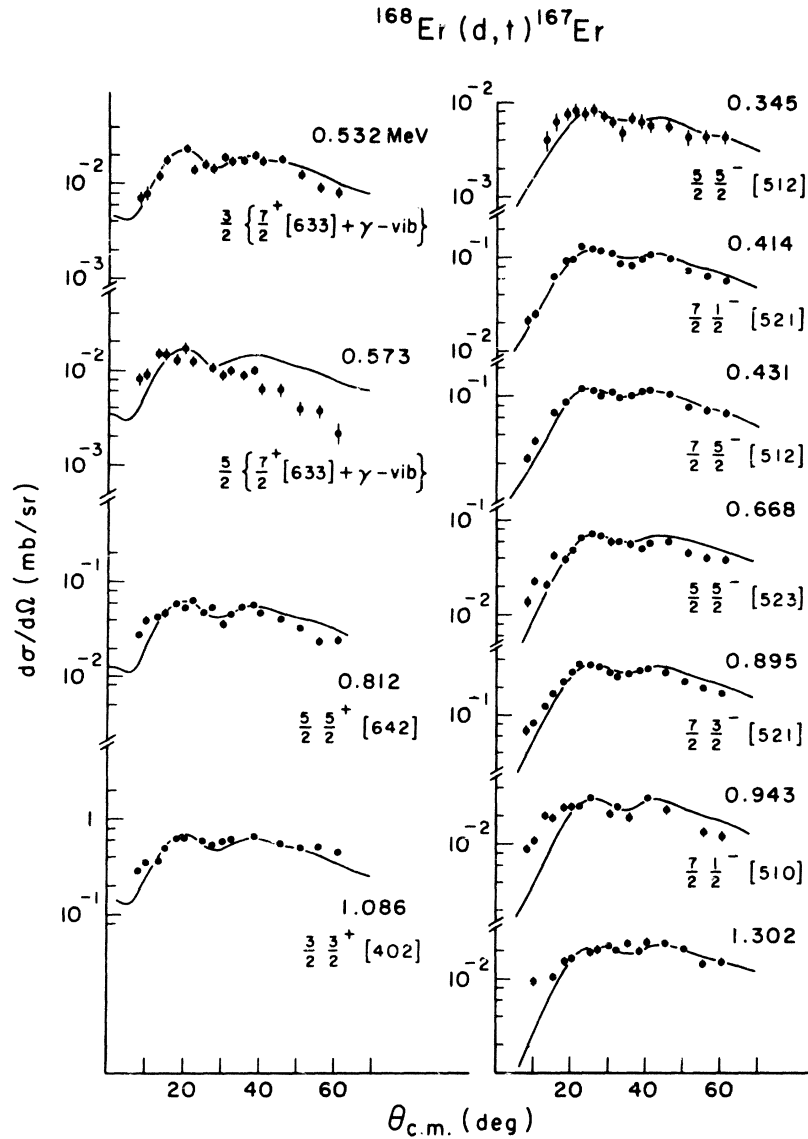


FIG. 3. $l=2$ and 3 angular distributions from the $^{168}\text{Er}(d,t)^{167}\text{Er}$ reaction at $E_d=17$ MeV. The solid curves are DWBA calculations.

Figure 5 shows the anomalous angular distributions (some of which have been identified in previous work with transitions to particular Nilsson model orbitals), whose angular distributions either

cannot be fitted by any DWBA calculation or can only be fitted with an l value which is incompatible with the Nilsson assignment. As discussed below, one of these anomalies can be attributed to a mis-

TABLE I. Optical model parameters and bound-state well parameters used in the DWBA calculation.

	V_r (MeV)	r_r (fm)	r_c (fm)	a_r (fm)	W (MeV)	W_D (MeV)	r_I (fm)	a_I (fm)	V_{s0} (MeV)	r_{s0} (fm)	a_{s0} (fm)	λ_{s0}
$^{168}\text{Er}+d^a$	102.2	1.15	1.15	0.81	...	17.6	1.34	0.68
$^{167}\text{Er}+t^b$	166.7	1.16	1.40	0.752	14.7		1.498	0.817
Bound states	c	1.25	1.25	0.65								25.0

^a Reference 20.

^b Reference 19.

^c Adjusted to give correct separation energy.

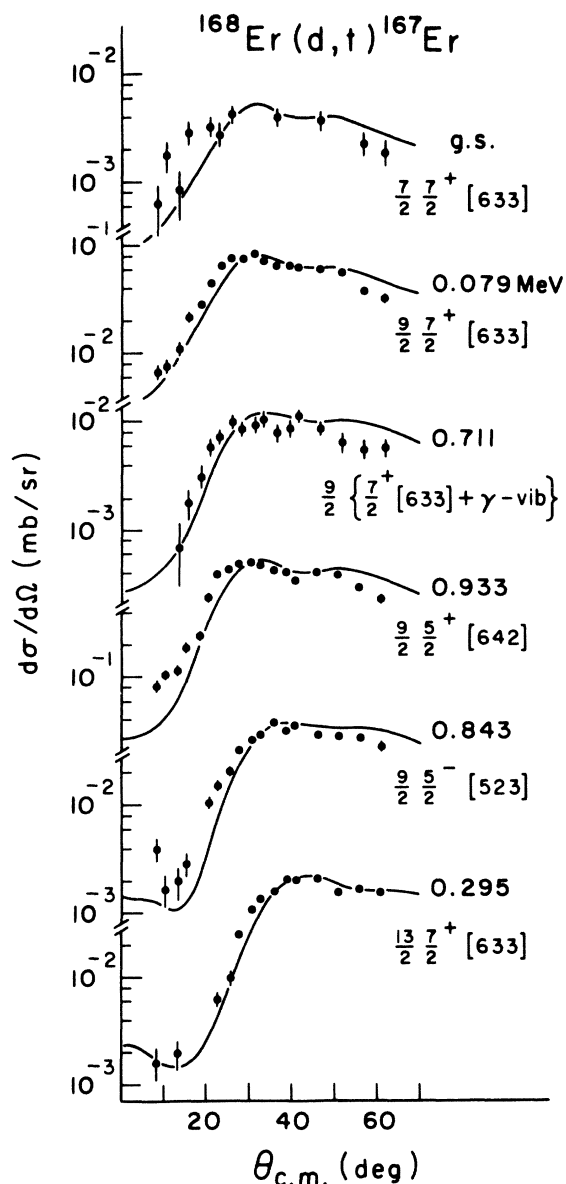


FIG. 4. $l \geq 4$ angular distributions from the $^{168}\text{Er}(d,t)^{167}\text{Er}$ reaction at $E_d = 17$ MeV. The solid curves are DWBA calculations.

assignment in the previous work; that is, the angular distribution for populating the 1.377 MeV state is very well fitted with a calculation which assumes an l value incompatible with the previous assignment of the state. But most of the anomalies in Fig. 5 almost certainly arise from transitions not susceptible to the assumptions underlying a normal DWBA analysis. These anomalous angular distributions exhibit several interesting characteristics: e.g., (1) 1.190 MeV state has strong oscillating structure, (2) 1.053 MeV state has very

large small angle cross sections, and (3) 0.281 state shows oscillating structure and large small-angle cross sections. Reaction mechanism effects which suggest explanations for these true anomalies will be discussed further below.

IV. SPECTROSCOPIC FACTORS AND NILSSON MODEL PARAMETERS

Spectroscopic factors have been extracted from the measured angular distributions by using the relation

$$\left(\frac{d\sigma}{d\Omega}\right)_{\text{exp}} = 3.33C^2S \frac{d\sigma/d\Omega_{\text{DWBA}}}{(2j+1)},$$

where C^2S is the spectroscopic factor, $(d\sigma/d\Omega)_{\text{exp}}$ is the measured cross section, $(d\sigma/d\Omega)_{\text{DWBA}}$ is the DWBA calculation made with the code DWUCK, and j is the angular momentum transfer assumed in the calculation. Table II lists, for each level populated in ^{167}Er , the excitation energy, empirically determined l value, Nilsson model assignment (where known from previous work), cross section at one angle, and spectroscopic factor. Spectroscopic factors have also been extracted for those levels whose angular distributions show significant deviations from DWBA predictions but whose l values have been suggested from previous Nilsson model assignments. These spectroscopic factors are clearly uncertain, representing a normalization of the DWBA prediction to the measured cross section in the angular region of the principal maximum in the DWBA angular distribution. As is discussed below and in the Introduction, the DWBA is used in these cases to help organize the data with no strong claim of validity for resulting spectroscopic implications.

Also shown in Table II are spectroscopic factors predicted by Nilsson model calculations²⁴ performed with the code BANDFIT.²⁵ Given an energy spectrum with spin, parity, and Nilsson model quantum numbers assigned to each level, this code will vary any or all of several parameters to fit the energy spectrum and then use the resulting parameters to predict spectroscopic factors for single-nucleon transfer reactions. As BANDFIT was used in this investigation, the parameters of the Nilsson deformed well were fixed at $\beta = 0.30$, $\mu = 0.42$, and $\kappa = 0.0639$.²⁶ The orbital population parameters (or pairing factors V_i^2) were constrained to satisfy the relation

$$V_i^2 = \frac{1}{2} \left(1 - \frac{\epsilon_i - \lambda}{[(\epsilon_i - \lambda)^2 + \Delta^2]^{1/2}} \right),$$

where $\epsilon_i - \lambda$ is the difference between the single-particle energy ϵ_i of the i th Nilsson orbital and the Fermi energy λ , and Δ is the pairing gap

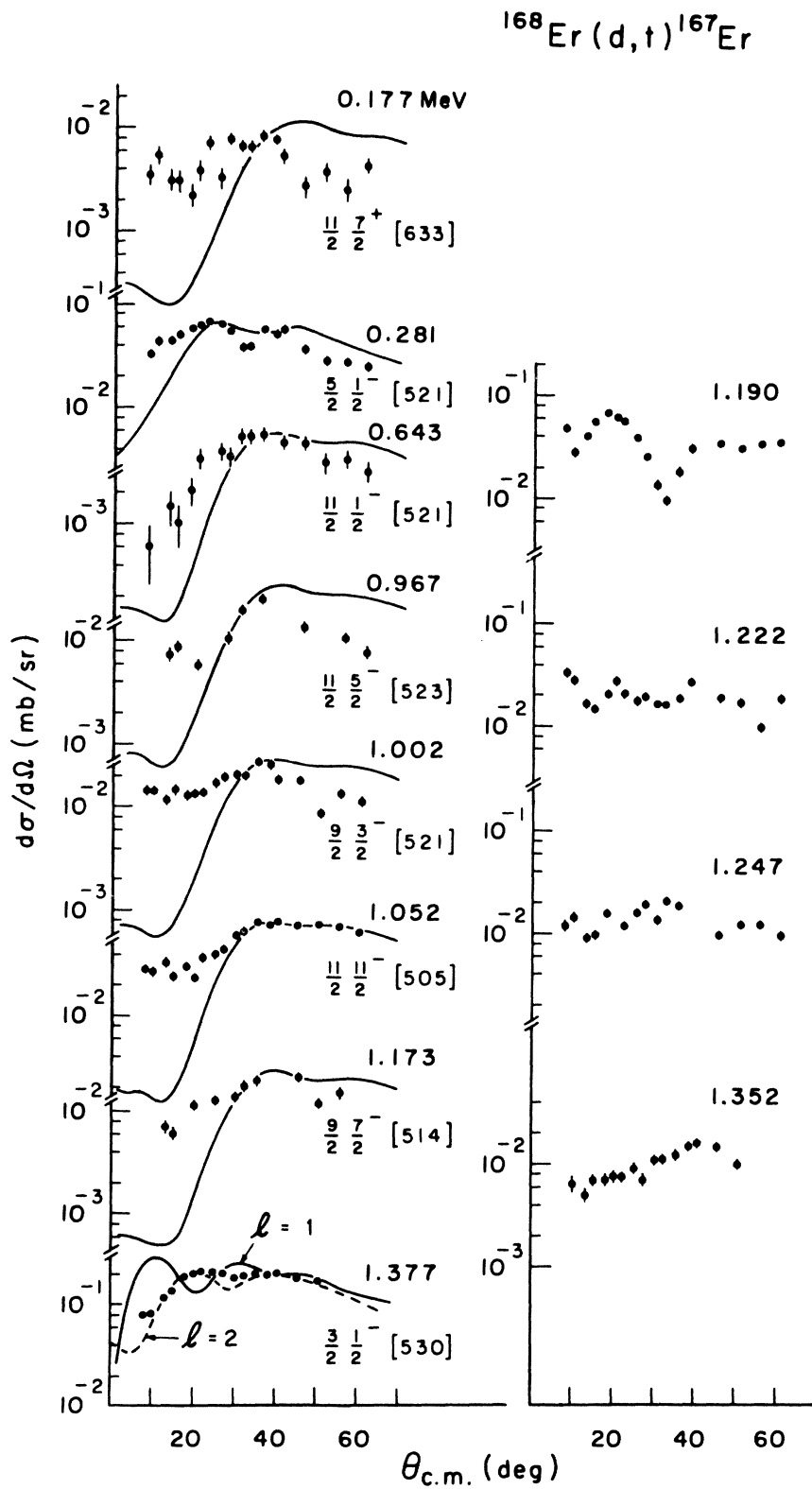


FIG. 5. Anomalous angular distributions from the $^{168}\text{Er}(d,t)^{167}\text{Er}$ reaction. The solid curves are DWBA calculations for an l value compatible with the indicated Nilsson model assignment. The dashed curve (discussed in text) is a DWBA calculation which assumes an l value which is incompatible to the Nilsson model assignment of the state.

TABLE II. Spectroscopic information for ^{167}Er levels populated through the $^{168}\text{Er}(d,t)^{167}\text{Er}$ reaction. Except for weakly populated states (cross sections $\leq 20 \mu\text{b}/\text{sr}$ in column 7) these excitation energies are accurate to ± 2 keV. Nilsson model assignments have been taken from Refs. 11, 14, and 35 except where otherwise indicated. Some states whose Nilsson assignments have been reported in previous work show angular distributions characteristic of l values incompatible with that l assignment: In these cases spectroscopic factors are shown for both possible l transfers.

E_x (MeV)	l	Nilsson model assignments	S_{exp}	S_{model}		$\frac{d\sigma}{d\Omega}(\theta=30^\circ)$ ($\mu\text{b}/\text{sr}$)
				Mixed	Unmixed	
0.000	4	$\frac{7}{2} \frac{7}{2}^+$ [633]	0.009	0.0008	0.006	5
0.079	4	$\frac{9}{2} \frac{7}{2}^+$ [633]	0.13	0.08	0.053	84
0.177	(6) ^a	$\frac{11}{2} \frac{7}{2}^+$ [633]	0.24	0.013	0.009	7
0.208	1	$\frac{1}{2} \frac{1}{2}^-$ [521]	0.19	0.12	0.12	47
0.264	1	$\frac{3}{2} \frac{1}{2}^-$ [521]	0.008	0.029	0.028	20
0.281	(3) ^a	$\frac{5}{2} \frac{1}{2}^-$ [521]	0.10	0.089	0.084	40
0.295	6	$\frac{13}{2} \frac{7}{2}^+$ [633]	1.22	1.47	0.94	42
0.345	3	$\frac{5}{2} \frac{5}{2}^-$ [512]	0.013	0.0002	0.0009	7
0.414	3	$\frac{7}{2} \frac{1}{2}^-$ [521]	0.14	0.20	0.10	115
0.431	3	$\frac{7}{2} \frac{5}{2}^-$ [512]	0.15	0.27	0.20	110
0.439	(5) ^b	$\frac{9}{2} \frac{1}{2}^-$ [521]	0.36	0.18	0.11	
0.532	2	$\frac{3}{2}^+$ c	0.022			190
0.573	2	$\frac{5}{2}^+$ c	0.014			9
0.643	(5) ^a	$\frac{11}{2} \frac{1}{2}^-$ [521]	0.063	0.041	0.013	7
0.668	3	$\frac{5}{2} \frac{5}{2}^-$ [523]	0.12	0.14	0.13	58
0.711	4	$\frac{9}{2}^+$ c	0.027			10
0.753	1	$\frac{3}{2} \frac{3}{2}^-$ [521]	0.21	0.13	0.14	500
0.802	1	$\frac{3}{2} \frac{1}{2}^-$ [510]	0.039	0.098	0.056	93
0.812	2	$\frac{5}{2} \frac{5}{2}^+$ [642]	0.054	0.004	0.005	35
0.843	5	$\frac{9}{2} \frac{5}{2}^-$ [523]	1.08	1.82	1.37	41
0.854	3 ^b	$\frac{5}{2} \frac{1}{2}^-$ [510]	0.042	0.051	0.041	
0.895	3	$\frac{7}{2} \frac{3}{2}^-$ [521]	0.53	1.01	0.95	290
0.911	c	$\frac{13}{2}^+$ b				
0.933	4	$\frac{9}{2} \frac{5}{2}^+$ [642]	0.28	0.17	0.20	120
0.943	3	$\frac{7}{2} \frac{1}{2}^-$ [510]	0.047	0.207	0.020	21
0.967	(5) ^a	$\frac{11}{2} \frac{5}{2}^-$ [523]	0.36	0.049	0.093	20
1.002	(5) ^a	$\frac{9}{2} \frac{3}{2}^-$ [521]	0.58	0.27	0.65	21
1.052	(5) ^a	$\frac{11}{2} \frac{11}{2}^-$ [505]	1.64	1.94	1.94	62
1.086	2	$\frac{3}{2} \frac{3}{2}^+$ [402]	0.91	1.74	1.56	570
1.109	6 ^b	$\frac{13}{2} \frac{5}{2}^+$ [642]	1.89	1.14	1.67	
1.135	0	$\frac{1}{2} \frac{1}{2}^+$ [400]	0.66	0.36	1.16	80
1.173	(5) ^a	$\frac{9}{2} \frac{7}{2}^-$ [514]	1.02	0.013	0.068	14
1.190	a					14
1.205	0		0.053			50
1.222	a					17

TABLE II. (Continued)

E_x (MeV)	l	Nilsson model assignment	S_{exp}	S_{model}		$\frac{d\sigma}{d\Omega}(\theta = 30^\circ)$ $\mu\text{b/sr}$
				Mixed	Unmixed	
1.247	a					14
1.280	b					
1.302	3		0.054			22
1.352	a					11
1.377	1	$\frac{3}{2} \frac{1}{2}^-$ [530]	(0.13)	0.23	0.27	175
	2		0.29			
1.426	0		0.14			130
1.440	0		0.015			16

^a Anomalous angular distributions shapes (see Fig. 5).

^b Populated weakly and/or obscured by stronger transitions so that no meaningful angular distribution could be extracted.

^c States reported in Ref. 15 to have large, vibrationally-mixed components.

V. DISCUSSION

As was mentioned in previous publications,⁸⁻¹⁰ it is difficult to separate the spectroscopic implications of the present measurements from those related to the reaction mechanism. There are several general cautions which should be noted prior to any further discussion of the spectroscopy and the reaction mechanism of (d, t) reactions on a deformed target like ^{168}Er .

The Nilsson model predictions of spectroscopic

factors are, in many cases, quite sensitive to the assumed Coriolis coupling strength. As discussed in Refs. 8-10, the observed energy spectra are not well reproduced unless these Coriolis matrix elements are reduced to ~60% of their values in the pure Nilsson model. This reduction has evolved from many experimental results²⁷ and has been further supported by the attempts of Damgaard, Jusuno, and Faessler²⁸ to explain backbending of yrast bands. This 60% reduction of the Coriolis coupling seems currently the most reasonable

TABLE III. Bandhead energy, moment of inertia parameters, decoupling constants, and level occupation parameters from fitting the energy spectra of ^{167}Er as described in the text.

Nilsson band	Bandhead energy (keV)	Moment of inertia (keV)	Decoupling constant	V_k^2
$\frac{7}{2}^+$ [633]	0	11.6		0.50
$\frac{9}{2}^+$ [624]	578	b		0.070
$\frac{5}{2}^+$ [642]	805	4.6		0.94
$\frac{3}{2}^+$ [402]	1087	0.41 ^{a,b}		0.96
$\frac{1}{2}^+$ [400]	1135	11.9 ^{a,b}	0.218	0.96
$\frac{1}{2}^-$ [521]	208	11.9	0.720	0.22
$\frac{5}{2}^-$ [512]	349	12.4		0.13
$\frac{5}{2}^-$ [523]	670	11.9		0.93
$\frac{3}{2}^-$ [521]	761	13.9		0.93
$\frac{1}{2}^-$ [510]	761	10.8	0.087	0.065
$\frac{7}{2}^-$ [514]	1045	13.2		0.04
$\frac{11}{2}^-$ [505]	1053	12.0		0.97
$\frac{1}{2}^-$ [530]	1282	18.2	0.600	0.97
$\frac{3}{2}^-$ [512]	1383	10.8		0.027

^a Strong $\Delta N = 2$ mixing makes these parameters very uncertain.

^b Not well determined because too few members of the band were observed.

procedure,²⁹ and there are equally great or greater discrepancies between the experimental spectroscopic factors and those from the fully-Coriolis-coupled Nilsson model calculations. However, this sensitivity of the model spectroscopic factors to the assumed strength of the Coriolis coupling adds another source of uncertainty to interpreting the spectroscopic factor discrepancies discussed below.

The model-predicted spectroscopic factors are even less reliable for the positive-parity bands which are subject to $\Delta N = 2$ mixing. This $\Delta N = 2$ mixing can become strong in ^{167}Er because two downward sloping (with increasing deformation) $N = 6$ orbitals, $\frac{1}{2}^+[660]$ and $\frac{3}{2}^+[651]$, encounter two upward sloping $N = 4$ orbitals, $\frac{1}{4}^+[440]$ and $\frac{3}{2}^+[402]$, just below the $N = 99$ Fermi surface.³⁰ The interactions between pairs of levels based on orbitals such as these have been studied³¹ but the resulting mixings are not at all well established. Also, the vibrational motions of the nuclear core can have a very important influence on the complicated nuclear structure in this mass region.³² The coupling of the vibrational and single-particle degrees of freedom can fragment the spectroscopic strength among several states in these deformed nuclides and, again, such effects are not understood in detail. Since multiquasiparticle components of the individual states cannot be populated by (d, l) transitions, disagreement between measured and calculated spectroscopic intensity patterns should be expected if vibrational coupling is important.

In addition to these features which complicate the calculation of Nilsson model spectroscopic factors, the DWBA analysis of the experiment is much less straightforward than it would be for a (d, l) reaction on a closed shell nucleus. As discussed in Refs. 8–10, the form factors used in the DWBA analysis were calculated with the spherical Woods-Saxon binding energy prescription (no configuration mixing). Such a procedure is only justifiable for a single particle outside a closed shell; normalizing such a wave function can change the magnitude of the form factor at the surface of a deformed nuclide by 30% or more.³³ But the conventional DWBA is used here to organize the experimental results of this investigation and further model-dependent adjustments of the form factors used in the analysis would be inappropriate.

The orbital angular momentum transfer, l , of a transition is assumed in this analysis to be determined if the measured angular distribution shape is well reproduced by the DWBA prediction for some l . This is not necessarily a compelling argument; multistep processes could yield an interference pattern resembling the DWBA pattern

for some l value. Such an effect has been reported for some $(^3\text{He}, t)$ transitions.³⁴ Ascuitto *et al.*¹ have reported oscillatory structure in angular distributions which, on the basis of CCBA calculations, they have attributed to multistep effects. Some of the effects discussed by Ascuitto *et al.* are sufficiently small that similar angular distributions are not classified as anomalous in this work where it has not been possible to perform CCBA calculations.

A. Spectroscopic information

The energy levels of ^{167}Er have previously been studied in considerable detail by (n, γ) , (d, p) , (d, t) , and $(^3\text{He}, \alpha)$ reactions.^{11–15, 32, 35} but no angular distributions for the transfer reactions have been obtained.

While the previous investigations are in substantial agreement as to the excitation energies of ^{167}Er states, there are some ambiguities of level identification, such as the 0.711, 1.086, 1.135, 1.205, and 1.440 MeV states which will be discussed below. Our angular distribution measurements supply further spectroscopic information by providing l values for the (d, l) transitions.

The detailed fitting of the ^{168}Er energy spectrum from Nilsson model calculations with Coriolis coupling has been discussed in Sec. IV. The Nilsson-assignments for the observed states listed in the second column of Table II have been taken from Refs. 11, 14, and 35. As discussed above, the calculated spectrum of odd-parity states agrees excellently with the experimental spectrum, but this is not the case for the even-parity spectrum.

Several transitions have an l value incompatible with the previous Nilsson assignments for their residual states. For instance the 1.377 MeV state, previously assigned $jk^\pi[Nn_z\Lambda] = \frac{3}{2}\frac{1}{2}^- [530]$ and thus expected to be a strongly populated hole state, has an $l = 2$ angular distribution shape. The 1.426 MeV excited state was assigned as $\frac{5}{2}\frac{1}{2}^- [530]$ and is found here to have $l = 0$. The 1.440 MeV state was assigned as $\frac{5}{2}\frac{3}{2}^- [512]$ and also is found here to be an $l = 0$ state. The 1.205 MeV state here is seen to be populated by an $l = 0$ transfer, while Kanestrom and Lovhoiden³⁵ assigned this 1.205 MeV state as $\frac{1}{2}\frac{5}{2}^+ [642]$ and Michaelis *et al.*¹⁴ had it as $\frac{7}{2}\frac{3}{2}^- [521]$ plus vibrationally mixed terms. Most probably these states were misidentified in the previous studies. The cross sections observed for these even- l transitions (to the 1.205, 1.377, 1.426, and 1.440 MeV states) may derive from the strength available in the $\frac{1}{2}^+[400]$, $\frac{1}{2}^+[660]$, and $\frac{3}{2}^+[402]$ rotational bands through mixing with other states.

The 1.053 MeV level was reported by Lovhoiden, Tjom, and Edvardson¹⁵ in their $(^3\text{He}, \alpha)$ measure-

ments to be $\frac{11}{2}^-\frac{11}{2}^-$ [505]. Also the 1.109 MeV level was shown¹⁵ to be $\frac{13}{2}^+$ which supported the $\frac{13}{2}^+\frac{5}{2}^+$ [642] assignment of this state.¹¹ Our Nilsson model calculations and experimental measurements indicate that the 0.812, 0.933, and 1.109 MeV states are the $\frac{5}{2}^+$, $\frac{9}{2}^+$, and $\frac{13}{2}^+$ members of the $\frac{5}{2}^+$ [642] rotational band.

The 0.711 MeV state is populated here in an $l=4$ transition in disagreement with the reports of Tveter and Herskind,¹³ Michaelis *et al.*,¹⁴ and Kanestrom and Lovhoiden,³⁵ who assigned this level as the $\frac{11}{2}^+$ state from the K_0+2 γ -vibrational band built on the ground state configuration. The population of the 0.711 MeV state by a (d,t) transition suggests the presence of some single-particle strength at this excitation energy, and the 0.711 MeV, $l=4$ state found here may not be the same state observed in the (n,γ) ¹⁴ and Coulomb excitation¹³ studies. Our Nilsson model calculations, which included the $\frac{9}{2}^+$ [624] configuration with $\frac{9}{2}^+$ and $\frac{11}{2}^+$ rotational members at 0.592 and 0.711 MeV, predicted these two states to be very weakly populated by (d,t) transitions. Indeed no 0.592 MeV state was populated in our spectrum and the 0.711 MeV state was $l=4$, not $l=6$. The Nilsson calculations also predicted the $\frac{13}{2}^+$ member of $\frac{9}{2}^+$ [624] rotational band at 0.829 MeV that was then impossible to trace because of two strong neighboring states at 0.812 and 0.843 MeV. This $\frac{13}{2}^+\frac{9}{2}^+$ [624] state has been reported to be at 0.826 MeV and to be populated by a (d,p) transition.³⁵ Our results, which assign the 0.532 MeV state as $\frac{3}{2}^+$, the 0.573 MeV state as $\frac{5}{2}^+$, the 0.711 MeV state as $\frac{9}{2}^+$, and the 0.911 MeV state as $\frac{13}{2}^+$, are consistent with the interpretation of Tjom and Elbek,¹¹ and Harlan and Sheline¹² that these above four states are members of the $(K-2)$ γ band built on the ground state with the admixture of the important intrinsic component $\frac{3}{2}^+$ [651].

The 1.302 MeV state, tentatively classified to be $l=3$, is the only odd-parity state which has not previously been identified. The rotational bands $\frac{7}{2}^+$ [633], $\frac{1}{2}^-$ [521], $\frac{5}{2}^-$ [512], $\frac{3}{2}^-$ [523], $\frac{3}{2}^-$ [521], and $\frac{1}{2}^-$ [510] are well interpreted. Though some members of these six rotational bands do have anomalous angular distributions without a clear transfer l value, it is believed that indirect transitions cause such effects instead of any misidentification of the Nilsson quantum numbers of the states.

Figure 6 compares the measured spectroscopic factors of the populated states with those predicted by the Coriolis coupled Nilsson model. The Nilsson bands in Fig. 6 are arranged in order of increasing quasiparticle energy. Spectroscopic factors marked with A in Fig. 6 correspond to transitions which exhibited anomalous angular distributions. As noted above, the results from fitting

the DWBA cross sections to the average level of the poorly fitted anomalous angular distributions are inherently most uncertain. Only two even-parity bands, $\frac{7}{2}^+$ [633] and $\frac{5}{2}^+$ [642], and included in Fig. 6 because the even-parity bands are well known to show strong $\Delta N=2$ mixing^{30,31} and are not well fitted in the Nilsson model calculations. The measured spectroscopic factors of all the observed even-parity states are listed in Table II.

The measured spectroscopic factors shown in Fig. 6 generally do not agree well with the predictions of the Coriolis coupled Nilsson model calculations. Michaelis *et al.*¹⁴ have done band-mixing studies in ^{167}Er (including Coriolis coupling and collective vibrations) and found a surprisingly large amount of mixing of collective vibrational strength. It is quite possible that the spectroscopic strength fragmentations are mainly due to the complicated mixings of these collective vibrations with quasiparticle degrees of freedom. Therefore, it is not surprising that the measured spectroscopic factors are not in good agreement with those of simple Nilsson model predictions. The interaction of quasiparticles with phonons gives rise to admixtures to the single-quasiparticle states and the extent of these admixtures should increase with the excitation energy as reported in Ref. 14. In this regard, an interesting pattern exists for the deviations of the measured and calculated spectroscopic factors for states which have been populated with substantial strength by (d,t) transitions. For the low excited bands $\frac{7}{2}^+$ [633] and $\frac{1}{2}^-$ [521] the deviations are $\leq 50\%$ while for the higher excited bands, the deviations are always $\geq 50\%$ (even up to more than 100% for the $\frac{3}{2}^-$ and $\frac{7}{2}^-$ members of the $\frac{1}{2}^-$ [510] band). This may quite reasonably indicate the tendency of vibrational motion to fragment the spectroscopic strength. Also Table III shows four $l=0$ transitions to states below $E_x=1.5$ MeV. There are only two available single-particle states ($\frac{1}{2}^+$ [400] and $\frac{1}{2}^+$ [660]) and these can provide only two $l=0$ transitions unless some residual interaction mixes them with other configurations. The additional two $l=0$ transfers are then believed to be further evidence of fragmentation due to particle-vibration coupling.

Table IV lists summed spectroscopic strengths for all observed l values of ^{167}Er . These have been compiled on the assumption that all Nilsson model assignments listed in Table II (third column)—including those levels discussed above as showing anomalous or incompatible l angular distributions—have been correctly identified. The measured spectroscopic factor sums agree well with the model calculated sums—surprisingly well since the spectroscopic strengths of individual transitions do not agree well at all. This may be

TABLE IV. Summed spectroscopic strengths of ^{167}Er for all observed l values. States identified in Table III with a rotational band built on a specified Nilsson level are assumed to have been correctly identified. Strengths of transitions to previously unidentified states whose angular distributions show characteristic l patterns have also been included. The model predictions include only the levels identified in Table III.

l	Calculated sum	Measured sum
0	1.160	0.849
1	0.377	0.488
2	1.744	1.375
3	1.967	1.248
4	0.251	0.472
5	4.313	4.493
6	2.625	3.460
Total	12.437	12.385

further evidence that considerable pickup strength is spread over many vibrationally coupled states.

B. Information from angular distribution shapes

It is obviously quite difficult to make a very clean separation of the effects observed in the present experiment into those whose implications are primarily spectroscopic and those whose implications most probably deal with the reaction mechanism. Just as the previous section of this paper dealt, after appropriate disclaimers, with new spectroscopic information arising from this investigation, this section deals with reaction mechanism information, subject to the following general cautions: (1) Owing to the fact that the fragmentation of single-hole strength discussed above is presumed to arise primarily from mixing of single-hole states with vibrational degrees of freedom, spectroscopic factors which severely disagree with Nilsson model expectations (Fig. 6 and Table III) are not presumed to imply any breakdown in the one-step direct reaction mechanism assumptions. Only anomalous angular distribution shapes are herein taken as evidence for more complicated mechanisms. This is clearly a conservative approach since CCBA calculations frequently produce angular distributions which strongly resemble DWBA predictions, differing only in absolute cross section.^{2,3} (2) Several of the angular distributions shown in Figs. 2–4 exhibit shape deviations from DWBA predictions which are probably significant and which are of the order of anomalies reported by Ascutto *et al.*¹ for $W(p, d)$ transitions. For example, in Fig. 2 the $l=0$ transitions show more pronounced oscillations at large angles than the DWBA predicts, and the $l=1$ transition to the 0.208 MeV state has small cross sections at large

angles when compared with DWBA predictions. Despite such clear differences in angular distribution shapes, the transitions shown in Figs. 2–4 are basically well fitted with DWBA angular distributions and are not regarded as anomalous in the discussion below. (3) Any of the anomalous angular distributions shown in Fig. 5, particularly for transitions to states at high excitation energy could possibly involve unresolved multiplets of states or, in the case of the 1.173 MeV state, be partially obscured by a neighboring strongly populated state. However, most of these transitions probably populate well-resolved states whose angular distributions are clearly anomalous—e.g., transitions to states at 0.177, 0.281, 1.052, and 1.190 MeV.

The anomalous angular distributions shown in Fig. 5, along with those reported in Refs. 9 and 10, provide strong evidence for a breakdown of one or more of the one-step direct reaction assumptions involved in performing a DWBA analysis. Six of these anomalous angular distributions have previously been identified with states which should be populated with high l transfer. In these cases the cross sections at small angles tend to be much larger than the DWBA predictions (e.g., the $\frac{11}{2}^{-}\frac{11}{2}^{-}[505]$ state at 1.052 MeV). It is plausible that two-step transitions could compete more favorably with the intrinsically weaker, large l direct transitions than with direct transitions populating states of low angular momentum. It is also plausible that the main effect of two-step competition in high l transitions would be a filling in of the DWBA-predicted small-angle minimum in the angular distribution because the competing two-step transition amplitudes would employ successive low- l steps which would individually tend to be forward peaked. These large cross sections at small angles for high- l transitions and the more oscillatory angular distributions for low- l transitions also shown in Fig. 5 are reminiscent of the very similar effects reported for (d, t) transitions populating states in ^{159}Gd , $^{161,163}\text{Dy}$ and ^{165}Er (Refs. 8–10); they are also similar to the results of (d, p) and (d, t) studies by several other authors on rare-earth targets.^{36–38}

There are several Nilsson bands for which at least one band member exhibits an anomalous angular distribution in at least four of the five residual nuclides: ^{159}Gd , $^{161,163}\text{Dy}$, $^{165,167}\text{Er}$.⁸ These bands are $\frac{11}{2}^{-}\frac{11}{2}^{-}[505]$, $\frac{5}{2}^{-}\frac{5}{2}^{-}[523]$, $\frac{1}{2}^{-}\frac{1}{2}^{-}[521]$, and $\frac{3}{2}^{-}\frac{3}{2}^{-}[521]$. As can be seen from Fig. 5, for $^{168}\text{Er} - ^{167}\text{Er}$ transitions some member of each of these bands exhibits an anomalous angular distribution: the band-head of the $\frac{11}{2}^{-}\frac{11}{2}^{-}[505]$ band, the $\frac{5}{2}^{-}$ and $\frac{11}{2}^{-}$ members of the $\frac{1}{2}^{-}\frac{1}{2}^{-}[521]$ band, the $\frac{11}{2}^{-}$ member of the $\frac{5}{2}^{-}\frac{5}{2}^{-}[523]$ band and the $\frac{3}{2}^{-}$ member of the $\frac{3}{2}^{-}\frac{3}{2}^{-}[521]$ band. It is obviously of interest to understand which direct

reaction assumptions fail so consistently for these particular Nilsson model configurations. The empirical trend is clear and follows the population of these levels through systems where their relation to the Fermi energy, and thus their single-hole spectroscopic strength, changes significantly and through isotone pairs where the overall density of levels changes significantly. An analysis of transitions to these bands with CCBA calculations is in progress, but preliminary calculations have not yet provided much insight into the problem.

VI. SUMMARY AND CONCLUSIONS

The measured angular distributions for (d, t) population of states in ^{167}Er are generally well fitted by DWBA calculations. However, a small but significant number of angular distributions are either completely incompatible with any DWBA calculation or only fitted by assuming an l transfer which is incompatible with the previously assigned angular momentum-parity of the residual state. Departure from a one-step direct reaction mechanism is suggested for the extremely anomalous cases while the latter cases are presumed to provide interesting spectroscopic information. A further trend in the evidence for the presence of

significant multistep transfer strength is the persistence throughout the $A \sim 160-168$ mass region of angular distribution shape anomalies in transitions to some members of the $\frac{1}{2}^-$ [521], $\frac{3}{2}^-$ [521], $\frac{5}{2}^-$ [523], and $\frac{11}{2}^-$ [505] bands.⁸⁻¹⁰

Several features of the present data suggest that vibration-hole coupling severely mixes single-hole strength over many states of ^{167}Er . Spectroscopic factors for transitions to individual states are in rather poor agreement with Coriolis-coupled Nilsson model predictions (even for negative-parity states), while the summed spectroscopic strength agrees well with Nilsson model expectations. Many more residual states are populated than should be possible (with direct reactions) unless the single-hole states mix with some other degree of freedom—e.g., there are four $l=0$ transitions resulting from only two $K = \frac{1}{2}^+$ states near the ^{168}Er Fermi surface.

ACKNOWLEDGMENTS

We appreciate the hospitality of Dr. J. R. Erskine in providing the code BANDFIT and allowing us to use the Argonne automatic plate scanner. We also acknowledge Dr. C. M. Vincent for several helpful discussions.

*Presently at University of Michigan, Ann Arbor, Michigan.

†Work supported by National Science Foundation.

‡Presently at Brookhaven National Laboratory, Upton, New York.

¹R. J. Ascutto, C. H. King, and L. J. McVay, *Phys. Rev. Lett.* **29**, 1106 (1972).

²R. J. Ascutto and N. K. Glendenning, *Phys. Rev.* **181**, 1396 (1969); N. K. Glendenning and R. S. Macintosh, *Nucl. Phys.* **A168**, 575 (1971).

³A. K. Abdallah, T. Udagawa, and T. Tamura, *Phys. Rev. C* **8**, 1855 (1973); D. K. Olsen, T. Udagawa, T. Tamura, and R. E. Brown, *ibid.* **8**, 609 (1973).

⁴N. Austern, *Direct Nuclear Reaction Theories* (Wiley-Interscience, New York, 1970), and references therein; S. K. Penny and G. R. Satchler, *Nucl. Phys.* **53**, 145 (1964).

⁵B. Elbek and P. J. Tjom, in *Advances in Nuclear Physics*, edited by M. Baranger and E. Vogt (Plenum, New York, 1969), Vol. III, and references therein.

⁶M. E. Bunker and C. W. Reich, *Rev. Mod. Phys.* **43**, 348 (1971).

⁷J. J. Kolata and J. V. Maher, *Phys. Rev. C* **8**, 285 (1973).

⁸J. V. Maher, G. H. Wedberg, J. J. Kolata, J. C. Peng, and J. L. Ricci, *Phys. Rev. C* **8**, 2390 (1973).

⁹J. C. Peng, J. V. Maher, G. H. Wedberg, and C. M. Cheng, *Phys. Rev. C* **3**, 1451 (1976).

¹⁰J. V. Maher, H. S. Song, G. H. Wedberg, and J. L. Ricci, *Phys. Rev. C* **14**, 40 (1976).

¹¹P. O. Tjom and B. Elbek, *K. Dan. Vidensk. Selsk. Mat.-Fys. Medd.* **37**, No. 7 (1969).

¹²R. A. Harlan and R. K. Sheline, *Phys. Rev.* **168**, 1373 (1968).

¹³A. Tveter and B. Herskind, *Nucl. Phys.* **A134**, 599 (1969).

¹⁴W. Michaelis, F. Weller, U. Fanger, R. Gaeta, G. Markus, H. Ottman, and H. Schmidt, *Nucl. Phys.* **A143**, 225 (1970).

¹⁵G. Lovhoiden, P. O. Tjom, and L. O. Edvardson, *Nucl. Phys.* **A194**, 463 (1972).

¹⁶J. R. Erskine and R. H. Vonderone, *Nucl. Instrum. Methods* **181**, 221 (1970).

¹⁷J. R. Comfort, ANL Physics Division Informal Report No. PHY-1970B, 1970 (unpublished); P. Spink and J. R. Erskine, ANL Physics Division Informal Report No. PHY-1965B (unpublished).

¹⁸P. D. Kunz, Univ. of Colorado (unpublished).

¹⁹E. R. Flynn, D. D. Armstrong, J. G. Beery, and A. G. Blair, *Phys. Rev.* **182**, 1113 (1969).

²⁰C. M. Perey and F. G. Perey, *Phys. Rev.* **132**, 755 (1963).

²¹J. M. Lohr and W. Haeberli, *Nucl. Phys.* **A232**, 381 (1974).

²²W. W. Daehnick and R. M. DeVecchio, *Phys. Rev. C* **11**, 623 (1975).

²³W. T. Pinkston and G. R. Satchler, *Nucl. Phys.* **72**, 641 (1965); R. J. Philpott, W. T. Pinkston, and G. R. Satchler, *ibid.* **A125**, 176 (1969), and references contained therein.

²⁴S. G. Nilsson, *K. Dan. Vidensk. Selsk. Mat.-Fys. Medd.* **29**, No. 16 (1955).

²⁵J. R. Erskine, Argonne National Laboratory (unpublished).

- ²⁶W. Ogle, S. Wahlborn, R. Piepenbring, and S. Fredriksson, *Rev. Mod. Phys.* 43, 424 (1971).
- ²⁷R. F. Casten, P. Kleinheinz, P. J. Daly, and B. Elbek, *Phys. Rev. C* 3, 1271; K. Dan. Vidensk. Selsk. Mat.-Fys. Medd. 38, No. 13 (1972), and references therein.
- ²⁸J. Damgaard, S. Jusuno, and A. Faessler, *Nucl. Phys.* A243, 492 (1975).
- ²⁹Aa. Bohr and B. R. Mottleson, *Nuclear Structure* (Benjamin, New York, 1975) Vol. II.
- ³⁰R. K. Sheline, M. J. Bennett, J. W. Dawson, and Y. Shida, *Phys. Lett.* 26B, 14 (1968); I. Kanestrom, P. O. Tjom, and J. Bang, *Nucl. Phys.* A164, 664 (1971).
- ³¹B. L. Anderson, *Nucl. Phys.* A196, 547 (1972), and references therein.
- ³²I. Kanestrom and P. O. Tjom, *Nucl. Phys.* A138, 177 (1969).
- ³³E. Rost, *Phys. Rev.* 154, 994 (1967).
- ³⁴R. A. Hinrichs, R. Sherr, G. M. Crawley and I. Proctor, *Phys. Rev. Lett.* 25, 829 (1970); P. G. Roos and C. D. Goodman, in *Nuclear Isospin*, edited by J. D. Anderson, S. D. Bloom, J. Cerny, and W. W. True (Academic, New York, 1969), p. 297.
- ³⁵I. Kanestrom and G. Lovhoiden, *Nucl. Phys.* A160, 665 (1971).
- ³⁶R. J. Ascutto, C. H. King, and L. J. McVay, *Nucl. Phys.* A226, 454 (1974).
- ³⁷R. H. Siemssen and J. R. Erskine, *Phys. Rev.* 146, 911 (1966).
- ³⁸M. Jaskola, K. Nybo, P. O. Tjom, and B. Elbek, *Nucl. Phys.* A96, 52 (1967); M. Jaskola and M. Kozłowski, *Acta Phys. Pol.* B3, 299 (1972).